Chapter 2
Grain Boundaries: Description, Structure and Thermodynamics

Grain boundary in a solid crystalline material is a region separating two crystals (grains) of the same phase. These two grains differ in mutual orientations and the grain boundary thus represents a transition region, where the atoms are shifted from their regular positions as compared to the crystal interior [12, 19, 20]. Grain boundaries represent the simplest interface: If the adjoining grains differ in chemical composition and/or in parameters of the crystal lattice, the interface between them is called *phase boundary* (*interphase boundary, heterophase boundary*). The grain boundary is also called *homophase boundary* in this classification. In general, interfaces represent a crystallographic and/or chemical discontinuity with an average width less than two atomic diameters [21, 22] although they may be sometimes more diffuse spreading over appreciable number of interplanar spacings [12, 23]. In this context, *free surface* is the interface between solid and vacuum [20].

Only those aspects of grain boundaries that are necessary for further reading will be mentioned in this chapter. For more thorough information other sources are recommended to the reader, especially the comprehensive book of Sutton and Balluffi [12] and selected parts of the book edited by Wolf and Yip [24].

2.1 Crystallographic Description of Grain Boundaries

To describe grain boundary crystallographically, a number of variables must be specified. Generally, the grain boundary can fully be characterised by five independent parameters (macroscopic degrees of freedom, DOFs), which provide us with information how to prepare the *bicrystal* (i.e. a sample containing two grains with the required orientation of the planar separating interface) from given single crystals (e.g. [12, 22, 25–27]). Three of them specify mutual misorientation of the adjoining grains A and B (Fig. 2.1). This misorientation is represented by a rotation, which brings both grains in perfect matching. It is defined by the rotation axis $\boldsymbol{o}$ (2 DOFs) and angle θ (1 DOF). Let us mention that there always exists at least one way how to describe such relationship in the case of non-enantiomorphic crystals. The orientation of the grain boundary between these misoriented grains is defined by the normal $\boldsymbol{n}$ to the grain boundary plane (2 DOFs).

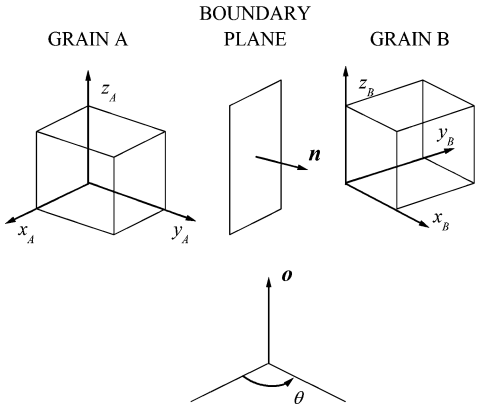

Fig. 2.1 Variables that define a grain boundary. x_A, y_A, z_A and x_B, y_B, z_B are the axes of the co-ordinates parallel to crystallographic directions in grains A and B, respectively. $\boldsymbol{o}$ is the rotation axis and θ is the rotation (misorientation) angle necessary to transfer both grains to an identical position. $\boldsymbol{n}$ determines the orientation of the grain boundary plane [20]

Following this characterisation, we can completely and unambiguously describe any grain boundary by the notation $\theta°[h_o k_o l_o], (h_{nA} k_{nA} l_{nA})$[1]. The grain misorientation is defined by the common axis $\boldsymbol{o} = [h_o k_o l_o]$, which is identical in both grains and expressed in a chosen co-ordinate system. The information about the grain boundary plane is related to one of these two grains only. From practical point of view, it is sometimes useful to identify the other part of the grain boundary, that is the joining plane related to the other grain, so that the boundary is described by $\theta°[h_o k_o l_o], (h_{nA} k_{nA} l_{nA})/(h_{nB} k_{nB} l_{nB})$. This notation represents an over-determination, indeed, but can give an easier and quicker view on the grain boundary crystallography.

It is necessary to add that besides the above mentioned five independent macroscopic DOFs, three other microscopic parameters exist that are represented by a vector $\boldsymbol{T}$ characterising a rigid body translation of both grains relatively one to the other, parallel and perpendicular to the grain boundary plane. The latter one represents, in fact, a volume expansion [28]. These translations are independent of macroscopic DOFs but controlled by the energetic reasons and cannot be chosen arbitrarily: for each grain boundary, few mutual translations may only exist that generate equilibrium atomic structures of the grain boundary under actual external conditions such as temperature, pressure and chemical composition. Thus, they cannot be considered as independent DOFs [12, 27, 29, 30].

Five DOFs that are necessary to describe completely the crystallography of a grain boundary imply existence of a huge number of different grain boundaries. Therefore, it is sometimes reasonable to categorise the grain boundaries into groups according to the relationships among individual DOFs. For example,

[1] In case of hexagonal structures, the notation should be modified according to the corresponding description of crystal planes and directions by four Miller indices.

the relationship between the rotation axis, $\boldsymbol{o}$, and the grain boundary normal, $\boldsymbol{n}$, leads to definition of the *tilt* grain boundaries ($\boldsymbol{o}\perp\boldsymbol{n}$) and the *twist* grain boundaries ($\boldsymbol{o}||\boldsymbol{n}$); the interfaces that do not fit with any of these relationships belong to the group of *mixed* grain boundaries [12, 19]. In the latter case, it is sometimes useful to find the tilt and twist components of the mixed relationship by imagining two successive rotations about perpendicular axes, one being located in the boundary plane, the other perpendicular to it [12]. When the boundary plane represents the plane of the mirror symmetry of the crystal lattices of two grains, it is described by the same Miller indices from the point of view of both adjoining grains. This boundary is called *symmetrical*. Its notation can be then simplified as $\theta°[h_o k_o l_o]$, $\{h_n k_n l_n\}$. The other grain boundaries are *asymmetrical*. Systematically, the categorisation of the grain boundaries can be represented by so-called *interface-plane scheme* based on relationship of the Miller indices of individual contacting planes 1 and 2 in a bicrystal and the twist angle φ of both planes as proposed by Wolf and Lutsko [31]. They distinguish four categories of grain boundaries

Symmetrical tilt grain boundary	$\{h_1k_1l_1\} = \{h_2k_2l_2\}$ and $\varphi = 0$
Asymmetrical tilt grain boundary	$\{h_1k_1l_1\} \neq \{h_2k_2l_2\}$ and $\varphi = 0$
Twist grain boundary	$\{h_1k_1l_1\} = \{h_2k_2l_2\}$ and $\varphi \neq 0$
Random (i.e. mixed) grain boundary	$\{h_1k_1l_1\} \neq \{h_2k_2l_2\}$ and $\varphi \neq 0$

Note that the mirror symmetry can be reached only at pure tilt grain boundaries. Let us mention that the last-mentioned grain boundary is called "random" or often "general": This brings terminological ambiguity, because the same terms are used to specify the character of the grain boundaries from the point of view of the properties (e.g. [12, 13, 20, 21, 32]). Therefore, we propose to call this class of the grain boundaries "mixed".

The above categorisation is, however, somewhat simplified and not unambiguous. From mathematical point of view, the total misorientation θ is given – in analogy to orientation matrix of a single crystal – by a 3×3 orthonormal matrix M. The matrix columns are the directional cosines of the crystal 2 in relation to the respective co-ordinates of the reference grain 1. Then the pair of the angle and axis is obtained from the matrix according to the relation [26]

$$\cos\theta = \frac{a_{11} + a_{22} + a_{33}}{2} \tag{2.1}$$

and the elements of the matrix M, a_{ij} $(i, j = 1, 2, 3)$, are related to the rotation axis $\boldsymbol{o}$ and its components o_i by

$$\boldsymbol{o} = o_1 : o_2 : o_3 = (a_{32} - a_{23}) : (a_{13} - a_{31}) : (a_{21} - a_{12}). \tag{2.2}$$

If $\theta = 180°$,

$$o_1 : o_2 : o_3 = (a_{11} + 1)^{1/2} : (a_{22} + 1)^{1/2} : (a_{33} + 1)^{1/2}. \tag{2.3}$$

Due to the symmetry of cubic structures, it is possible to describe the same boundary by 24 various but equivalent notations and characters [12]. These notations result from the product of the symmetry matrices T_i with M [26]

$$M' = T_i M, \tag{2.4}$$

where $i = 1, 2, \ldots, 24$ in cubic structures. The 24 matrices determine 24 pairs of the rotation axis and misorientation. For example, the same interface characterised as 36.87°[100]{013} *symmetrical tilt grain boundary* can also be described as 53.13°[100]{013} *symmetrical tilt grain boundary* or 180°(013) *twist grain boundary* [20, 33, 34], etc. Although all descriptions are entirely equivalent, the lowest-angle solution or lowest-index rotation axis is conventionally used for description of the grain boundary (i.e. 36.87°[100]{013} in the above example). This notation will also be used throughout this work. For detail crystallographic description of the grain boundaries, the reader is referred to more thorough papers dealing with the systematic of grain boundaries, for example to Sutton and Balluffi [12], Randle [22, 26, 35], Wolf [29] and Wolf and Merkle [36].

2.2 Atomic Structure of Grain Boundaries

As was mentioned above, individual atoms in the grain boundary core are shifted from their regular crystal positions as compared to the crystal interior. Then, a question arises: How are the atoms arranged there? The early models assumed that the grain boundaries are amorphous (e.g. [37], cf. also [19]). Amorphous layers as an equilibrium arrangement of silicon atoms at the grain boundaries also resulted from recent computer simulations [38–40], although they could exist obviously only in a metastable state [41]. Later, the grain boundary was considered as composed of the regions of the "good" and "bad" material [42]: this idea was developed in the dislocation models of the grain boundary structure [25]. At present, however, it is undoubtedly established that the structure of grain boundaries is crystal like [28–31]. This model is strongly supported by theoretical as well as experimental evidences of anisotropic behaviour of grain boundaries (e.g. [12, 20, 21, 43–46]). From the point of view of actual atomic structure, two groups can be distinguished, *low-angle grain boundaries* and *high-angle grain boundaries*. Let us notice that we can meet dual terminology in the literature corresponding to these groups (a) *low-angle* and *high-angle* grain boundaries (e.g. Gleiter and Chalmers [21], Wolf and Merkle [27], McLean [19], Smith [46], Flewitt and Wild [47]) and (b) *small-angle* and *large-angle* grain boundaries (e.g. Sutton and Balluffi [12], Cahn [39], Gottstein and Shvindlerman [48], Finnis and Rühle [49]). In the present work, the terminology of type (a) is used.

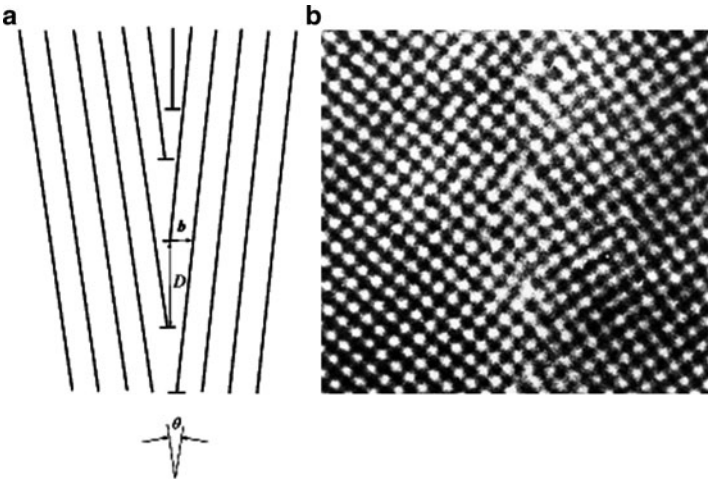

Fig. 2.2 Structure of a low-angle grain boundary (**a**) schematic illustration, (**b**) image of a [100] low-angle grain boundary in molybdenum revealed by the high-resolution electron microscopy. The distance between individual atoms is about 0.2 nm. (J.M. Pénisson, with permission)

2.2.1 Low-Angle Grain Boundaries

When the angle θ between two adjoining grains is low enough, this misorientation can be accommodated by an array of dislocations [12, 50, 51]. It is well known that equilibrium arrangement of discrete dislocations (so called *primary grain boundary dislocations*) with Burgers vector $\boldsymbol{b}$ having the same sign can be represented by a periodic row (wall) as it is shown in Fig. 2.2. Tilt grain boundaries are formed by edge dislocations, while twist grain boundaries consist of an array of screw dislocations.

The angle θ is related to the size of the Burgers vector $|\boldsymbol{b}|$ and the dislocation spacing D by the expression

$$\sin\frac{\theta}{2} = \frac{|\boldsymbol{b}|}{2D}. \tag{2.5}$$

For low θ, $\sin(\theta/2)$ can be approximated by $\theta/2$ and thus, $\theta \approx |\boldsymbol{b}|/D$.

The energy of a low-angle grain boundary can simply be derived on basis of the theory of elastic continuum. The energy of an edge dislocation can be expressed as

$$E_{\mathrm{ed}} = \frac{\mu \boldsymbol{b}^2}{4\pi(1-\nu)} \ln\frac{D}{r_0} + E_{\mathrm{c}}, \tag{2.6}$$

where μ is the shear modulus, ν is the Poisson ratio, r_0 and E_{c} are the radius and the energy of the dislocation core. Supposing that $r_0 \approx |\boldsymbol{b}|$ and that the number of dislocations per unit length in the low-angle grain boundary is $n = 1/D \approx \theta/|\boldsymbol{b}|$,

we can write the energy of a low-angle tilt grain boundary per unit area as

$$\sigma_{\mathrm{LATGB}} = \frac{\theta}{|\boldsymbol{b}|}\left[\frac{\mu \boldsymbol{b}^2}{4\pi(1-\nu)}\ln\frac{1}{\theta} + E_{\mathrm{c}}\right] = \theta(A - B\ln\theta), \tag{2.7}$$

where $A = E_{\mathrm{c}}/|\boldsymbol{b}|$ and $B = \mu|\boldsymbol{b}|/4\pi(1-\nu)$ [25].

With increasing θ, D decreases to such an extent that dislocations loose their character and the dislocation theory cannot be further used to describe the grain boundary structure. Generally, it is assumed that the limit for successful application of the dislocation model lies between 13° and 15° [52] that corresponds approximately to the value $D \approx 4|b|$. This limit has been supported experimentally: For example, measurements of the contact angle at the grain boundary trace at free surface in bismuth showed the transition between low-angle and high-angle grain boundaries at 15° [53]. Recently, the measurements of migration of planar grain boundaries in aluminium showed a sharp limit between low-angle and high-angle $\langle 112\rangle$ and $\langle 111\rangle$ tilt grain boundaries at 13.6° [54].

2.2.2 High-Angle Grain Boundaries

Overcoming the above-mentioned limit of the misorientation angle between two adjoining grains, the dislocation model of the grain boundary structure fails because individual dislocations are no more distinguishable and overlap one with the other. As a result, the angular dependence of grain boundary energy does not fit with the course proposed by (2.7). Systematic computer modelling of numerous grain boundaries in face-centred cubic (fcc) crystals [55–60] resulted in development of the *structural unit model* to describe atomic arrangement of the high-angle grain boundaries [55–66]. According to this model, a high-angle grain boundary is formed by repeated structural units that represent particular arrangements of limited number of atoms. In fact, only a few types of basic structural units exist [43, 46, 66–68] and therefore, there is a limited number of grain boundaries formed exclusively by single structural units. Ashby et al. [66] describe seven different convex polyhedra – tetrahedron, regular octahedron, pentagonal bipyramid, tetragonal dodecahedron, capped trigonal prism, capped Archimedian prism and icosahedron – as basic objects forming the structural units. The structures of the majority of grain boundaries consist of combinations of the simple structural units. Between two *delimiting* grain boundaries formed by single structural units of the types $|A|$ and $|B|$, the structural units of the other grain boundaries will be described as $|A_x B_y|$ to accommodate corresponding misorientation angle θ [12]. Examples of the structures of high-angle grain boundaries obtained by computer modelling are depicted in Fig. 2.3. Here, three [100] symmetrical tilt grain boundaries in the body-centred cubic (bcc) structure are shown, the {013} delimiting grain boundary (structural unit of type $|A|$), the {024} delimiting grain boundary (structural unit of type $|B.B|$), and the {037} grain boundary. As it is apparent, the structure of the latter grain

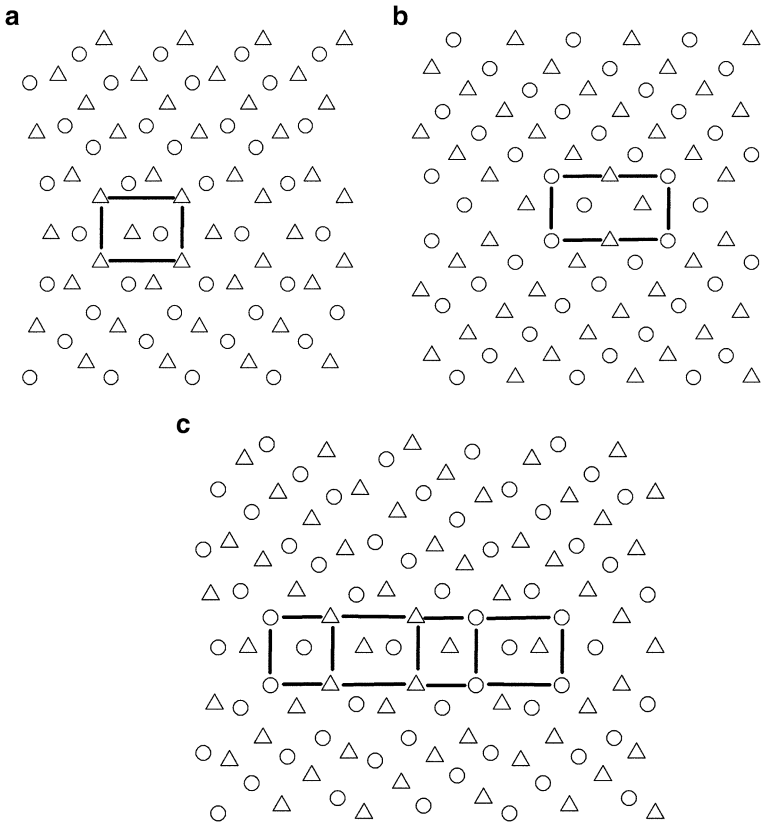

Fig. 2.3 Structure of three [100] symmetrical tilt grain boundaries in a bcc bicrystal (**a**) {013}, (**b**) {024}, (**c**) {037}. *Circles* and *triangles* represent two parallel (100) planes [20]. (According to J. Erhart)

boundary is formed by combination of structural units of neighbour delimiting grain boundaries, {013} and {024}, according to the scheme $|AA| + |B.B| \rightarrow |AB.AB|$. This scheme copies the combination of Miller indices of the grain boundary planes, $\{013\} + \{024\} \rightarrow \{037\}$ [20]. Since the atomic arrangement of the grain boundary differs from that of the bulk crystal, the grain boundary possesses higher energy as compared to the crystal interior. A low energy of the grain boundary suggests that this arrangement is close to that of crystal interior. The (delimiting) grain boundaries consisting of single structural units and exhibiting sharp minima at energy–orientation dependence are called *singular* [12]. An example of the atomic structure of a singular grain boundary is shown in Fig. 2.4. The high-energy grain boundaries are then called *general*. Their structure is composed of combination of two or more structural units of singular grain boundaries (cf. the {037} grain boundary in Fig. 2.3). There is another group of grain boundaries representing transition in energetic behaviour of singular and general grain boundaries, so called *vicinal*

Fig. 2.4 Atomic structure of the 70.5° [110], {112} symmetrical tilt grain boundary in molybdenum. The spacing between parallel rows of atoms is 0.25 nm. The *bright belt* in the *centre* of the image is computer-simulated structure [69]. (T. Vystavěl, with permission)

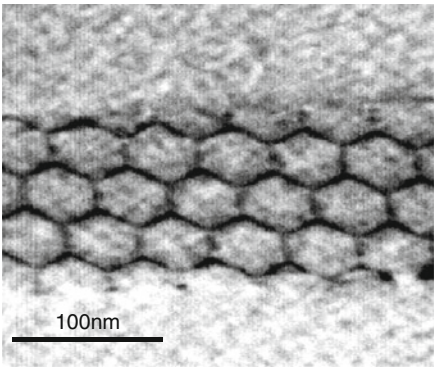

Fig. 2.5 Array of screw dislocations in the tilt grain boundary in molybdenum vicinal to the 70.5° [110], {112}. Transmission electron microscopy [69]. (T. Vystavěl, with permission)

grain boundaries [12, 70]. The structure of a vicinal grain boundary is composed of the structural unit of the closest singular grain boundary modified by an array of *secondary grain boundary dislocations* (low-angle grain boundary) [12]. An example of such dislocation array is shown in Fig. 2.5. The combination of the single structural unit and the dislocation array transforms to the structural unit of a general grain boundary at much lower misorientations from the singular grain boundary than it corresponds to the limit of existence of low-angle grain boundaries 10–15°. Because the Burgers vectors of the secondary grain boundary dislocations for positive and negative deviations from the singular orientation may be different, the cusps on the structural dependence of grain boundary energy (and other interface properties) can be asymmetric [71].

In addition to the categories of grain boundaries described above, we can often find in literature the term *special* grain boundaries (e.g. [21, 27, 32, 47, 72]). This term denotes those grain boundaries that exhibit sharp extremes at any property–orientation dependence, for example, fracture toughness, diffusivity, propensity for segregation, migration rate, sliding rate as well as corrosion rate. It is expected that each singular grain boundary is special albeit not vice versa. Sometimes, we can also find – mainly in earlier sources – the term *random* grain boundaries (e.g. [21, 32]) as a synonym for *general* grain boundaries. The term "general grain boundaries" is

more straightforward when related to the behaviour of the interface. Speaking about the occurrence of the grain boundaries in a material, the term "random" can be used to document randomness of nucleation of individual grains in cast material.

2.3 Classification of High-Angle Grain Boundaries

In Sect. 2.2.2, the high-angle grain boundaries were classified into singular, vicinal and general. Although numerous computer simulations and experimental studies revealed some of the singular grain boundaries, their complete set has not been unambiguously established until now. This set can differ according to the lattice structure, type of material, etc. Therefore, a large effort has been paid to develop a simple geometrical classification of grain boundaries to specify the grain boundaries of singular (special) character. Let us summarise here the most important attempts.

2.3.1 Coincidence-Site Lattice Model

Historically, the first model used for identification of special grain boundaries, the *coincidence-site lattice* model, was proposed in 1949 by Kronberg and Wilson [73]. It is based on simple assumption that the grain boundary energy is low when the coincidence of atomic positions in both adjoining grains is high because the number of bonds that are broken across the boundary is small [74]. This is understandable if we accept that the minimum Gibbs energy of the system corresponds to the state of perfect arrangement of the atoms in the lattice positions. Therefore, a grain boundary will possess lower energy when more atoms will coincide with the positions of the perfect crystal than in a non-coincident state. Let us assume that two grains are misoriented by a chosen angle θ around a chosen axis $\boldsymbol{o}$. At superposition of these crystals some atomic sites coincide: such sites are called *coincidence sites*. They are spread regularly throughout the whole superimposition and create a superlattice called *coincidence-site lattice* (CSL). A two-dimensional (2-D) example of the CSL is shown in Fig. 2.6. In 3-D space, the CSL in cubic structures is frequently tetragonal.

It is apparent from Fig. 2.6 that in 36.87° [100] misorientation relationship, each fifth position is the coincidence site. The density of coincidence sites, or better, its reciprocal value Σ is an important parameter characterising the CSL. Choosing an elementary cell, we can determine the value of Σ as

$$\Sigma = \frac{\text{number of coincidence sites in an elementary cell}}{\text{total number of all lattice sites in an elementary cell}}. \tag{2.8}$$

In cubic lattices, it can simply be evaluated from the Miller indices of the symmetrical tilt grain boundary corresponding to a given misorientation [75],

$$\Sigma = \delta(h^2 + k^2 + l^2), \tag{2.9}$$

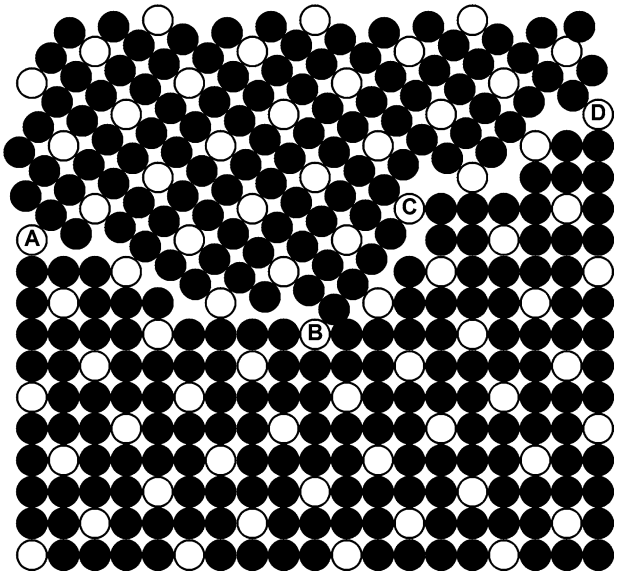

Fig. 2.6 Geometric model of the 36.87° [100] tilt bicrystal with simple cubic lattice. The *circles* represent the positions of individual atoms in misoriented crystals, the *empty circles* denote the coincidence sites. The orientation of the grain boundary varies from {013} symmetrical (A–B), through (001)/(034) asymmetrical (B–C) to {012} symmetrical (C–D) [20]

where $\delta = 1$ if $(h^2 + k^2 + l^2)$ is odd and $\delta = 1/2$ if $(h^2 + k^2 + l^2)$ is even because in cubic systems, all Σ values are odd [76]. For example, the symmetrical grain boundaries in the 36.87° [100] misorientation relationship of the two grains in Fig. 2.5 are {013} and {012}. Both combinations of Miller indices result in value $\Sigma = 5$. Sometimes, a parameter Γ is used defined as surface density of the density of coincidence sites in the grain boundary plane [77].

It is apparent that orientation dependence of Σ is not monotonous. There alter misorientations characterised by low values of Σ with those possessing high values. Since the ideal crystal can be displayed as a bicrystal with 0° misorientation, each atomic position in its overlapping superlattice is the coincidence site and thus, $\Sigma = 1$. The interfacial energy of an imaginary grain boundary in such misorientation relationship (i.e. a crystal plane) is naturally equal to zero and this "interface" can be considered as singular grain boundary. Various experiments proved that the twin grain boundaries in both bcc and fcc structures characterised by the value $\Sigma = 3$ are singular. Similarly, special behaviour was often detected for the grain boundaries characterised by low values of Σ (e.g. [32,48,72,78]). Therefore, it has widely been accepted that *low value of* Σ *indicates special grain boundary*.

Due to the purely geometrical character of CSL it is clear that any small change of grain misorientation from the singular grain boundary results in drastic change in coincidence and consequently, in corresponding change of the value of Σ. On the other hand, it usually does not bring substantial change of the properties of the grain boundary because its structure is changed by introducing individual dislocations. It

is thus reasonable to relate the character of such (vicinal) boundaries to the basic singular one and to define the range of existence of low-Σ CSL relationship despite small deviations from the true coincidence. This range of existence of low-Σ CSL relationship is characterised by the maximum angular deviation, v_{m}, which is supposed to conserve its character by addition of an array of secondary grain boundary dislocations. The density of dislocations is then related to Σ [79]. The relationship between v_{m} and Σ is usually introduced rather empirically,

$$v_{\mathrm{m}} = \frac{v_0}{\Sigma^{\xi}}. \tag{2.10}$$

Generally, it is mostly accepted that $v_0 \approx 15°$ represents the angular limit for low-angle grain boundary so that all low-angle grain boundaries are described as $\Sigma = 1$. The mostly adopted Brandon criterion [80] uses the value $\xi = 1/2$, while other authors proposed to use other values, for example Ishida and McLean [81] the value of $\xi = 1$, Deschamps et al. [82] the value of $\xi = 2/3$ and Palumbo et al. [83] the value of $\xi = 5/6$.

As mentioned above, Σ is strictly geometric criterion [49,78] and its value characterises exclusively mutual misorientation of two adjoining crystals. We can see in Fig. 2.6 that CSL gives no information on actual grain boundary orientation or on its atomic structure: the grain boundary plane changes its orientation while the value of Σ remains constant. This is the reason why Σ often fails as the characteristic parameter for classification of grain boundaries [12, 71, 84, 85]. For example, the spectrum of the $\Sigma = 5$, 36.9°[100] tilt grain boundaries includes not only the {012}, {013} and (011)/(017) special grain boundaries but also the (0 3 11)/(097) and (018)/(047) general ones [86]. In turn, a typically non-coincidence relationship 45°[100]($\Sigma \to \infty$) includes also the special (001)/(011) grain boundary [87]. Despite this basic failure, however, the CSL approach is still used to characterise individual grain boundaries in the concept of Grain Boundary Engineering (e.g. [32,88], see Chap. 7) and in many structural studies [89,90] although other schemes were proposed for classification of grain boundaries (e.g. [12,84]).

Let us notice that the 45°[100] grain boundaries belong among the irrational or incommensurate interfaces [91]. The symmetrical tilt grain boundary corresponding to this misorientation relationship can only be described as {0 kl}, since the ratio of the Miller indices k and l is irrational, $k/l = \sqrt{2}$.

The CSL concept is sometimes generalised, and considered as the *O-lattice* [75] or the DSC-lattice[2] (DSCL). O-lattice, which has been used mainly to analyse the dislocation structure of grain boundaries, is defined as the space array of coincidence points of two interpenetrating misoriented lattices of grains A and B albeit not only atomic sites. A grain boundary can be geometrically constructed by discarding atoms of lattices A and B and the points of registry in the boundary will be given by the intersections of the grain boundary plane with the O-lattice. Similarly to CSL model, O-lattice is independent of the position of the grain boundary. For

[2] DSC: Displacement Shift Complete.

a chosen misorientation of the two grains, there exists a large number of O-lattices due to a variety of transformations of the space lattice of one grain to that of the other grain. Each point of the O-lattice can serve as an origin of this transformation [88]. Therefore, the O-lattice is a "lattice of origins" (O for Origin) [49]. From this point of view, the CSL is a sublattice of the O-lattice. The periodicity of the structure of the boundary does not coincide with the period of the O-lattice but with that of the CSL. The advantage of the O-lattice is that it is a continuous function of the transformation relating the nearest neighbour atoms of space lattices of grains A and B. In contrast to CSL, the spacing of the O-lattice thus varies continuously with misorientation of the two grains.

DSCL was proposed to describe isolated dislocations and steps on grain boundaries [75]. In fact, small misorientation from ideal CSL relationship does not bring a dramatic change of the coincidence but this deviation is compensated by periodic arrangement of dislocations. These dislocations need to have Burgers vectors that conserve the original CSL relationship when forming a low-angle grain boundary (in fact, this is concept of vicinal grain boundaries). In this way, the energy of the grain boundary increases. There are rather small vectors that conserve the CSL relationship – the vectors of the DSCL. Supposing two misoriented grains A and B, the DSCL is defined as the grid including all points of grains A and B, that is by the minimum displacement vectors preserving the CSL relationship. DSCL, thus, defines all relative displacements of these two grains supposing the overall pattern of atoms produced by the interpenetrating space lattices to remain unchanged. These patterns conserve the displacements: any displacement of the space lattice of the one grain relatively to the other one by a DSCL vector defined by the DSCL represents a complete pattern shift. Additionally, each vector joining the points of misoriented space lattices of grains A and B is a vector of the DSCL [49, 92]. It is worth noting that the DSCL vectors define the possible Burgers vectors of the grain boundary dislocations, which may appear in its structure [49]. Another important property of the DSCL is that the interplanar spacing in direction perpendicular to the misorientation axis varies with decreasing CSL spacing. It means that the degree of coincidence of two misoriented grains decreases with reducing DSCL vectors. The subject of the O-lattice and the DSCL approach is treated in detail elsewhere [12, 93].

2.3.2 Interplanar Spacing

Another geometrical parameter that was applied to characterise individual grain boundaries is *interplanar spacing* $d(hkl)$. Interplanar spacing is defined as the shortest distance between two parallel crystal planes (hkl) and can be simply evaluated. For example, for cubic structures we can express $d(hkl)$ as

$$d(hkl) = a\frac{\varepsilon}{\sqrt{h^2 + k^2 + l^2}}, \tag{2.11}$$

where a is the lattice parameter and $\varepsilon = 1/2$ or 1 depending on the particular combination of odd and even Miller indices of the grain boundary plane [27]. When considering the asymmetrical interfaces, the effective interplanar spacing is used averaging $d(hkl)$ of both component boundary planes

$$d_{\text{eff}} = \frac{d(h_1k_1l_1) + d(h_2k_2l_2)}{2}. \tag{2.12}$$

High values of the ratio d/a correspond to densely packed boundary planes and are accepted to indicate special interfaces [20].

A comparison of the dependence of the standard enthalpy, ΔH_{P}^0, (see Chap. 4) of phosphorus grain boundary segregation in α-iron [94] on d_{eff}/a and Σ is shown in Fig. 2.7. We can see that high values of d_{eff}/a characterise special tilt grain boundaries much better than low values of Σ [20, 95].

To be rigorous, anisotropic grain boundary properties should be correlated to the *relative grain boundary volume* $\delta V/A$ [96]. Unfortunately, there is only little information about this quantity from computer simulations as well as from high-resolution electron microscopy observations so that this kind of correlation has not been done yet. Therefore, the first rough approximation for the correlation of grain boundary properties such as solute segregation, to $d(hkl)/a$ and/or to d_{eff}/a seems to be quite promising.

Let us mention that d_{eff}/a similarly to Σ, is exclusively a geometrical parameter and does not reflect completely the specific properties of grain boundaries. Although it seems to classify the tilt grain boundaries in a better way than Σ, it completely fails in case of twist grain boundaries when any misorientation around a chosen axis provides identical value of d while both the grain boundary properties and the value of Σ change [70, 96].

2.3.3 Hierarchy of Grain Boundary Planes

Based on analysis of numerous experimental data and results of computer simulations, Paidar [84, 97] proposed a geometrical classification of tilt grain boundaries according to hierarchy of their planes. In principle, it is based on the scheme of formation of structural units of individual grain boundaries as was suggested in Sect. 2.2.2. In case of symmetrical grain boundaries, the hierarchy starts at the "ideal" singular grain boundaries such as {001} and {011}. Supposing the 2-D space (i.e., [100] misorientation), these interfaces are the starting interfaces. Due to their exclusivity, they may be ascribed to the 0th *classification level* (CL). Combining them (in relation to bcc structure) according to the "reaction"

$$\{002\} + \{011\} \rightarrow \{013\}, \tag{2.13}$$

the grain boundary corresponding to the first CL is specified. As it was already mentioned in Sect. 2.2.2, this "reaction" is accompanied by the combination of structural

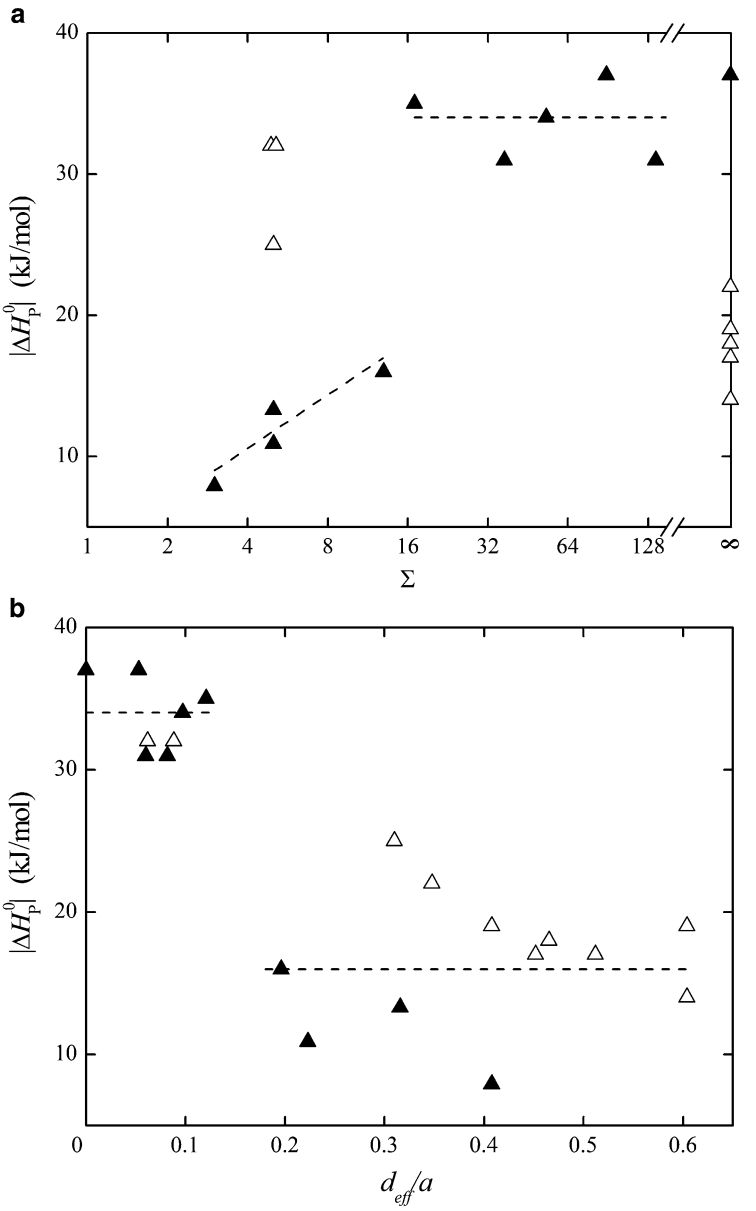

Fig. 2.7 Dependence of absolute value of enthalpy of phosphorus segregation at grain boundaries of α-iron, $|\Delta H_P{}^0|$, (**a**) on reciprocal density of coincidence sites Σ, and (**b**) on effective interplanar spacing, d_{eff}/a, [20,95]. *Solid symbols* depict symmetrical grain boundaries, *empty symbols* denote asymmetrical grain boundaries. Low values of Σ and high values of d_{eff}/a should indicate special grain boundaries

units of the grain boundaries of the 0th CL. In case of the {013} grain boundary, however, a new simple structural unit is formed and therefore, this grain boundary is considered as singular.

Combination of the grain boundary plane belonging to the first CL with the neighbour grain boundary planes of the lower CL gives

$$\{002\} + \{013\} \rightarrow \{015\} \tag{2.14}$$

and

$$\{013\} + \{011\} \rightarrow \{024\}. \tag{2.15}$$

{015} and {012} (which are considered as identical with the {024}) are the grain boundary planes corresponding to the second CL. As was shown above, the {012} grain boundary also possesses its own structural unit and is singular. Further application of the proposed scheme leads to identification of the grain boundary planes of the third CL,

$$\{002\} + \{015\} \rightarrow \{017\}, \tag{2.16}$$

$$\{015\} + \{013\} \rightarrow \{028\}, \tag{2.17}$$

$$\{013\} + \{024\} \rightarrow \{037\} \tag{2.18}$$

and

$$\{024\} + \{011\} \rightarrow \{035\}. \tag{2.19}$$

This scheme can continue by specifying the grain boundary planes of higher CLs. In this way, each [100] tilt grain boundary can be classified. Similarly, applying this scheme onto the whole 3–D space of orientations, all grain boundaries can be specified. All grain boundaries belonging to the CLs 1–4 in cubic structures are listed in Table 2.1.

It is demonstrated above, for example for the {037} grain boundary plane, that the structural unit of this grain boundary is composed of the structural units of the grain boundaries from the lower CL, that is this grain boundary is considered as general. The main message that we can draw from this scheme is that *singular grain boundaries belong to the lowest CLs*: *Once a plane of a general grain boundary appears in the hierarchy, the resulting grain boundaries on the higher CLs cannot be singular* [84]. It was also shown that there is a close relationship between this hierarchy and the value of d/a [84]. On the other hand, the relationship between this hierarchy and the value of Σ is not straightforward (cf. Table 2.1). Although this hierarchy well reflects formation of structural units of individual grain boundaries, it is not unambiguously determined which CL represents the border between the singular and general grain boundaries. Nevertheless, the grain boundary plane hierarchy offers a clear instruction where the singular grain boundaries can be found.

As regards asymmetrical tilt grain boundaries, singular interfaces should be exclusively formed by the planes of singular symmetrical grain boundaries [97]. Let us represent the orientation of the asymmetrical grain boundaries by the map

Table 2.1 Classification of symmetrical tilt grain boundary planes [84, 97]

CL	fcc structure		bcc structure	
	Plane	Σ	Plane	Σ
1	{111}	3	{112}	3
2	{113}	11	{123}	7
	{133}	19	{013}	5
	{012}	5	{111}	3
			{114}	9
3	{112}	3	{134}	13
	{115}	27	{235}	19
	{122}	9	{012}	5
	{155}	51	{015}	13
	{013}	5	{113}	11
	{023}	13	{116}	19
	{135}	35	{233}	11
			{334}	17
			{124}	15
4	{117}	51	{145}	21
	{114}	9	{257}	39
	{337}	67	{358}	49
	{335}	43	{347}	37
	{355}	59	{035}	17
	{377}	107	{037}	29
	{144}	33	{014}	17
	{177}	99	{017}	25
	{034}	25	{338}	41
	{035}	17	{3 3 10}	59
	{025}	29	{115}	27
	{014}	17	{118}	33
	{179}	131	{122}	9
	{157}	75	{455}	33
	{124}	21	{556}	43
	{357}	83	{223}	17
	{123}	7	{129}	43
	{159}	107	{127}	27
	{139}	91	{138}	37
	{137}	59	{147}	33
	{134}	13	{136}	23
			{124}	21
			{349}	53
			{237}	31
			{239}	47
			{457}	45
			{345}	25
			{356}	35

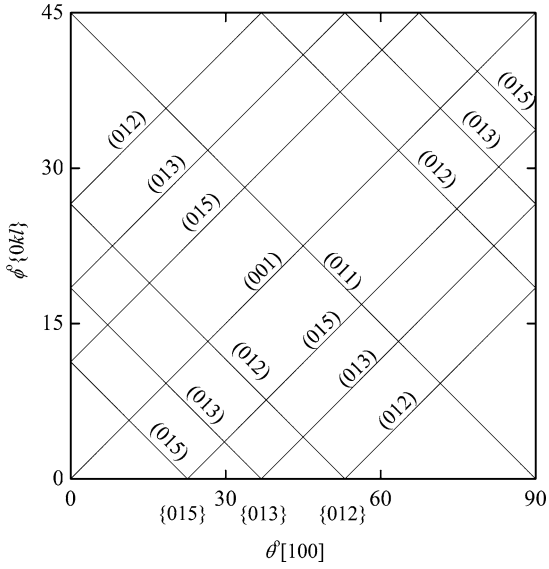

Fig. 2.8 Orientation map of [100] tilt grain boundaries in cubic structures. θ is the misorientation angle between two adjoining grains, ϕ is the deviation of the grain boundary plane from the chosen symmetrical orientation. The *lines* parallel to the *diagonals* denote the grain boundaries having one of the planes identical [94, 95]

shown in Fig. 2.8. Here, the angle θ means the misorientation angle between two adjoining grains and the angle ϕ is the deviation of the grain boundary plane from the chosen symmetrical position (for [100] tilt grain boundaries in cubic structures $0 \leq \theta \leq 90°, 0 \leq \phi \leq 45°$). The lines parallel to the diagonals in this plot represent the grain boundaries in which one of the planes is kept identical. According to this scheme and accepting that the {012}, {013} and {015} grain boundaries are singular [94], singular asymmetrical grain boundaries are expected to be formed by mutual combinations of the (001), (011), (012), (013) and (015) planes.

Recently, this classification of asymmetrical tilt grain boundaries was proved experimentally by measurements of anisotropy of grain boundary segregation of phosphorus, silicon, and carbon in bcc iron [94, 95, 98–100]. These experiments showed, that besides the {013}, {012} and {015} symmetrical tilt grain boundaries that belong to the first, second and second CLs (Table 2.1), respectively, the (001)/(013) grain boundary and all boundaries containing the (011) boundary plane exhibit special behaviour (Fig. 2.9). It means that all symmetrical grain boundaries denoted as singular were found to exhibit special segregation behaviour. In the case of asymmetrical tilt grain boundaries, the combinations of the lowest CL planes, (011)/(001), (011)/(013) and (001)/(013) were found to form special grain boundaries, too. Therefore, these grain boundaries can be considered as singular. In addition, all other asymmetrical grain boundaries formed by the (011) grain boundary plane were found to be special albeit they may not be all singular. Similarly, all asymmetrical grain boundaries formed by the (001) grain boundary plane exhibit segregation behaviour, which can be characterised as "transition", that is they can be considered as kind of "vicinal" grain boundaries. The segregation experiments leading to this conclusion will be discussed in Chap. 5 in more detail.

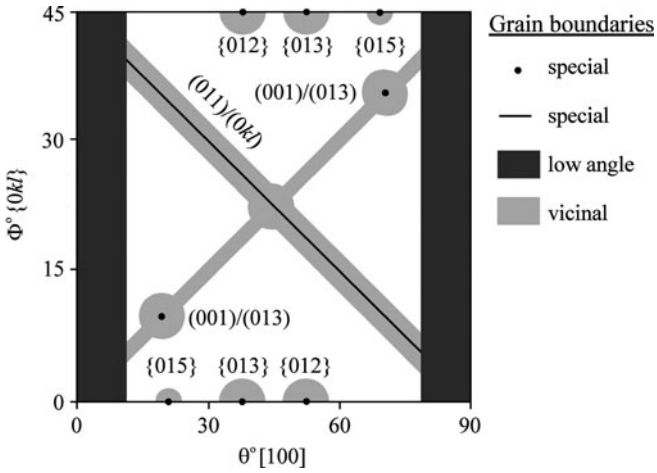

Fig. 2.9 Schematic map of character of [100] tilt grain boundaries in bcc iron, indicated by different shadings and symbols. *Black line* and *points* refer to the special grain boundaries. *Light grey* area depicts vicinal grain boundaries and *dark grey area* does low-angle interfaces. All boundaries in the white area are general interfaces. The orientations in the map are defined in Fig. 2.8 [94, 95]

2.4 Basic Thermodynamics of Grain Boundaries

Since the grain boundaries represent one type of general interfaces, their thermodynamic treatment should be consistent with the general thermodynamics of interfaces, for example with thermodynamics of free surfaces that is thoroughly developed [12]. On the other hand, each interface has its own specifics that should also be taken into account. In contrast to free surfaces, there is much larger variety of different grain boundaries due to presence of the other crystal in contact with the grain "surface" in the grain boundary in comparison to vacuum in case of the free surfaces.

However, the grain boundaries represent a non-equilibrium crystal defect and thus, it may seem questionable whether the equilibrium thermodynamics can be principally applied to describe their states and processes. In contrast to equilibrium point defects (vacancies and interstitials) that can simply be equilibrated due to local fluctuations, the grain boundaries represent extended defect, which can be only removed by application of external forces. For example, grain boundaries form a 3-D network throughout a polycrystal that is additionally pinned at free surfaces: this network represents a stable object characterised by a local minimum of an appropriate potential and therefore, its components such as grain boundaries can be treated thermodynamically [48, 72].

The first thermodynamic description of interfaces was proposed by Gibbs [101]. His treatment is based on construction of a "dividing surface" between the interface and bulk crystal, which has to be later subtracted from the values of the thermodynamic parameters [12]. This rather laborious treatment was replaced by an

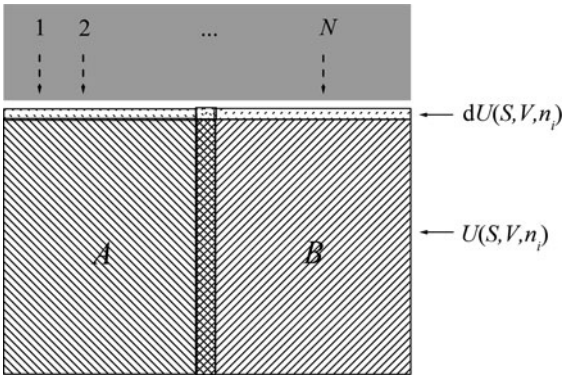

Fig. 2.10 A growing bicrystal for introduction of the grain boundary energy

equivalent but more straightforward one developed by John Cahn [102, 103]. For introduction of thermodynamic functions of grain boundaries, we will adopt his modern formalism [12, 102].

To introduce thermodynamic state functions of grain boundaries, let us consider an open system composed of two N-component grains A and B of an identical phase differing exclusively in orientations that are separated by a planar grain boundary (bicrystal, Fig. 2.10). If this bicrystal grows as a result of equilibrium transport of components $1, 2, \ldots, N$ from reservoirs under constant temperature T, hydrostatic pressure P and chemical potentials μ_i of each component $i = 1, 2, \ldots, N$, the increase of the internal energy of the system can be expressed as [12],

$$\mathrm{d}U = T\mathrm{d}S - P\mathrm{d}V + \sum_{i=1}^{N} \mu_i \mathrm{d}n_i + \sigma \mathrm{d}A, \tag{2.20}$$

where S is the entropy of the system, V is its volume, n_i is the amount of the component i ($i = 1, 2, \ldots, N$) and A is the grain boundary area. σ is the *grain boundary internal energy per unit area* (of the grain boundary) and represents the change of the internal energy of the closed system with the change of grain boundary area at constant entropy and volume [102, 103],

$$\sigma = \left(\frac{\partial U}{\partial A}\right)_{S,V,n_i}. \tag{2.21}$$

Adopting the fundamental relationship among the thermodynamic state functions U, H (enthalpy), F (Helmholtz energy) and G (Gibbs energ) [104], $H = U + PV$, $F = U - TS$, $G = U + PV - TS$, we can additionally express the grain boundary energy as

$$\sigma = \left(\frac{\partial F}{\partial A}\right)_{T,V,n_i}, \tag{2.22}$$

or

$$\sigma = \left(\frac{\partial H}{\partial A}\right)_{S,P,n_i}, \tag{2.23}$$

or

$$\sigma = \left(\frac{\partial G}{\partial A}\right)_{T,P,n_i}. \tag{2.24}$$

Equation (2.24) gives probably the most important representation of the grain boundary energy per unit area as the change of the Gibbs energy of the system with the change of the grain boundary area under constant temperature and pressure in a closed system.